SEMI-ANNUAL PROGRESS REPORT

1 September 1969 - 30 April 1970

Sponsored by

Advanced Research Projects Agency

ARPA Order No. 1244
Program Code No. 8D10

CONTRACTOR:	Engineering Experiment Station University of Arizona Tucson, Arizona 85721
EFFECTIVE DATE:	1 July 1968
CONTRACT EXPIRATION DATE:	28 February 1971
AMOUNT OF CONTRACT:	$179,733.00
CONTRACT NO.:	F33615-68-C-1707, Sub-Item 1AA
PRINCIPAL INVESTIGATORS:	Robert H. Chambers Professor of Physics 602-884-2776 Stuart A. Hoenig Professor of Electrical Engineering 602-884-1617
TITLE:	New Techniques in Nondestructive Testing by Acoustical and Exo-electron Emission

ACOUSTICAL EMISSION STUDIES

ROBERT H. CHAMBERS

Co-Principal Investigator

The purpose of this report is to describe recent investigations of the frequency distribution of acoustical emission from growing fatigue cracks in 24-ST aluminum sheet. The fatigue cracks were introduced by a high-amplitude, low-cycle bending mode of deformation. Figure 1 shows a schematic representation of the mode of bending and the placement of the PZT-5, 9.7-MHz transducers. A Hewlett-Packard spectrum analyzer was used in the zero sweep mode to record the emission events. The resulting signals were recorded on the persistent screen scope face and photographed later. The acoustical emission was stimulated by high stress amplitude oscillations of the specimens. As the introduced cracks grew in response to external driving stress, they produced bursts of acoustical emission that looked like sharp spikes on the scope face.

Figure 2 shows a typical pulse amplitude *vs.* time diagram taken from a polaroid photograph of the scope face. The time scale is 5 seconds per division. The external stress applied to the sample was oscillated at $\sim$ 1/2 cycle per second; therefore emission bursts appear about every one second, corresponding to maximum crack growth on each

maximum half cycle. Figure 2 represents the acoustical emission output due to growing cracks as seen through the rather narrow band-pass filter of the Hewlett-Packard spectrum analyzer, in this particular case, a center frequency of ∿ 5 KHz and a band width of 50 Hz.

Figures 2 through 15 represent the amplitude *vs.* time plots for different settings of the center frequency, but for each setting the bandwidth was selected so as to have the same ratio to the center frequency, namely f(center)/Δf(bandwidth) = 100. About one hundred specimens were oscillated to fracture in this manner, giving results typified by those shown in Figures 2 through 15.

Several features are immediately evident: (1) at the lowest frequencies there is very little activity at the earliest times following the initial introduction of a crack; (2) at frequencies in the vicinity of 200 to 700 KHz there is early acoustical emission activity; and (3) there is relatively little activity beyond 3 MHz at any time. The large rise in pulse amplitude at 9.7 MHz is due to the stimulation of the longitudinal resonance of the PZT-5 transducer used in this investigation; it is relatively flat from 10^5 Hz to nearly 6 MHz, rising only at the fundamental longitudinal 9.7 MHz resonance and the third harmonic at 29.1 MHz. No emission was observed at the third harmonic.

It is instructive to cross-plot the curves in Figures 2 through 15 in the following manner: Consider the number of times pulses occur

in the range from A_1 to A_2, A_2 to A_3, *etc.*, in a particular time range, say five seconds after the fatiguing cycles begin. Each of these numbers is then compared for each frequency measured, and a composite spectrum is assembled for several times during the terminal fatigue experiment. Figure 17 shows the composite spectrum for two times: *early* and *late* where *early* corresponds to the interval of time from 0 to 5 seconds after the beginning of the deformation, and *late* corresponds to approximately the last five cycles before final fracture.

Two points should be noted in Figure 17: (1) the early spectrum is peaked in the 500-KHz range; and (2) the late spectrum begins to look like the spectrum for a simple pulse, *i.e.*, the lower frequency components have started to increase, whereas the early spectrum looks more like a relatively narrow range of frequencies characteristic of "ring down" behavior.

The spectra of Figure 17 are interpreted as follows: At the early stage there are many small cracks that are beginning to open and enlarge. These cracks can vibrate with frequencies in the low MHz range. Their ring down behavior should show as a band of frequencies. Furthermore, since there are many cracks randomly opening, the pulses should occur over a fairly broad time range. As the small cracks enlarge, their characteristic frequencies should decrease. Also, as the smaller cracks intercept one another, fewer but larger

cracks should be formed creating fewer but larger amplitude pulses in time. Finally, a large central crack should dominate giving a relatively sharp, well-defined pulse as it extends to final fracture. The last stage should have the narrowest time distribution but the broadest frequency distribution.

To investigate this hypothesis further, a detailed study was made of the time domain structure of the acoustical emission pulses from the early through the late stages. Figures 18 through 30 show how the time domain structure does in fact change as the late stage is reached. Figure 18 shows a typical burst taken at a moderate sweep speed with the analyzer set at a center frequency of 300 KHz and a bandwidth of 30 KHz. Notice the very complicated structure when viewed with this increased resolution. Now as we progress toward the later stages, it is evident that the pulses are narrowing down considerably, requiring a greater sweep speed in order to resolve them. Finally, in the late stage the pulses are over 10 times as narrow as in the early stage. Qualitatively, then, our hypothesis concerning the interpretation of the progression of microcracks growing into macrocracks and producing a characteristic frequency spectrum appears to hold up when investigated in the time domain as well.

The method used here to investigate the frequency spectrum of growing fatigue cracks is very time consuming. It has only statistical validity since we require the use of a number of samples and must make

a cross plot to obtain the spectrum. Clearly, it is better to obtain the spectrum of a single pulse directly instead of having to investigate the average behavior of a large number of pulses. To this end we are hoping to apply the newly designed 10-channel single-pulse spectrum analyzer to the problem of analysis of fatigue crack emission. The analyzer is in the last stages of construction and testing and should be available for actual crack analysis soon.

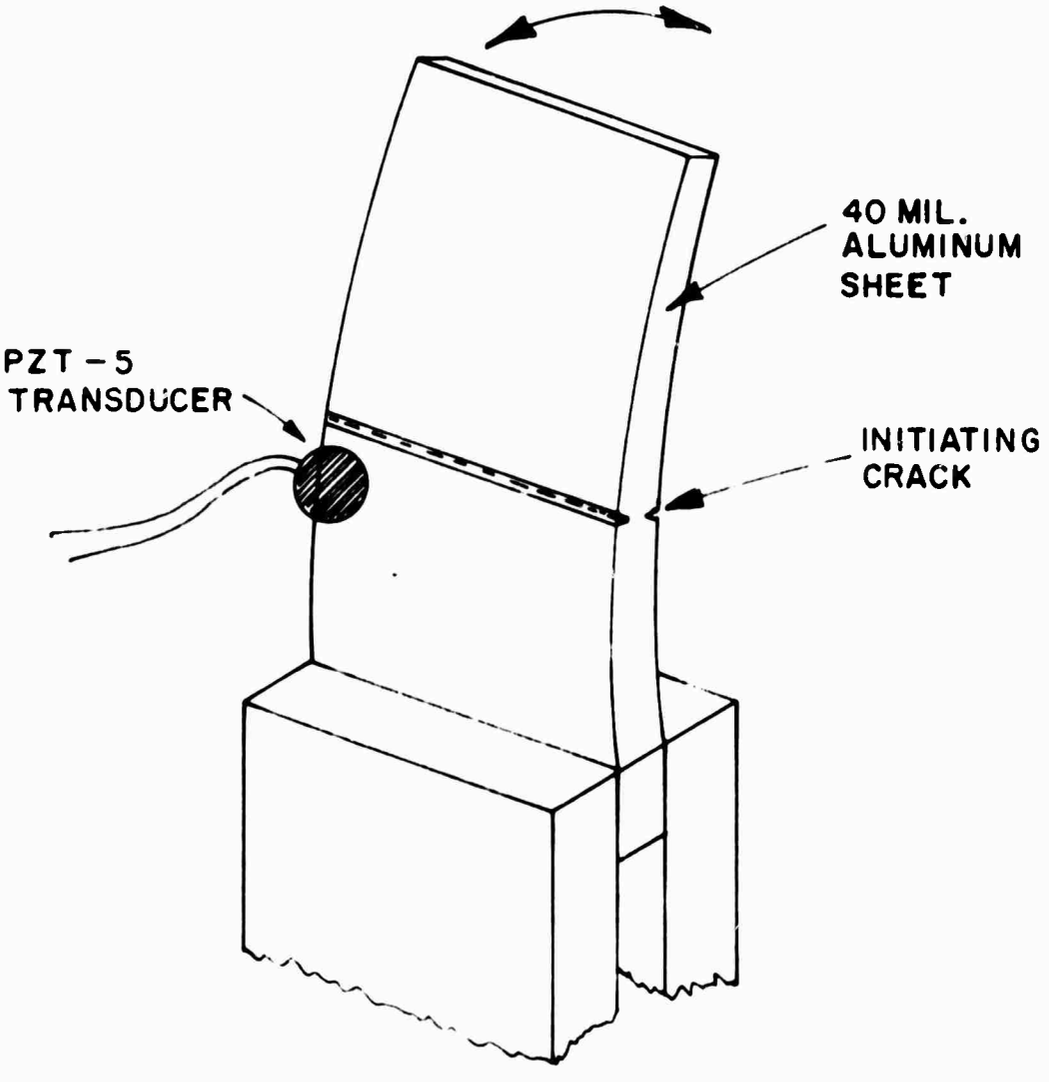

Figure 1. Schematic of bend type fatigue sample showing placement of transducer and initiating fatigue crack.

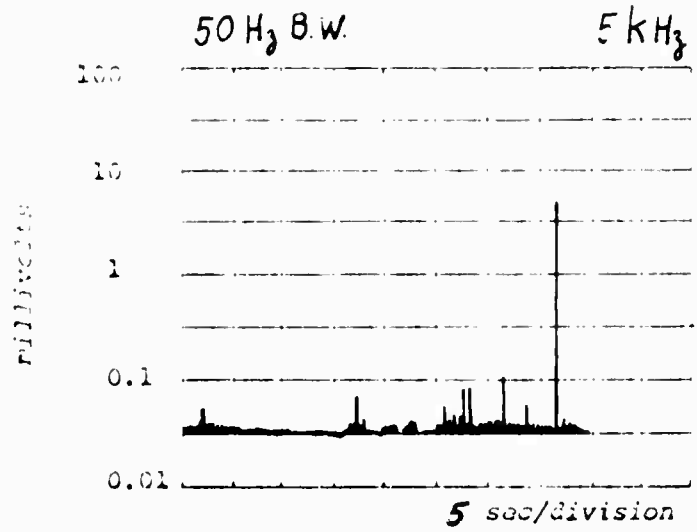

Figure 2. Acoustical emission output vs. time for low cycle high amplitude fatigue experiment as observed through a 5 KHz, 5 Hz bandwidth filter. Stress cycle rate: 1/2 Hz.

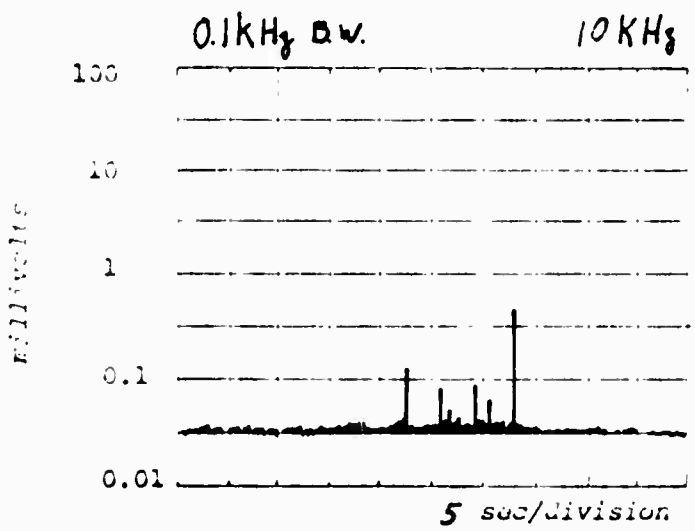

Figure 3. Emission output vs. time similar to that in Figure 2, but observed through a 10 KHz, 0.1 KHz bandwidth filter.

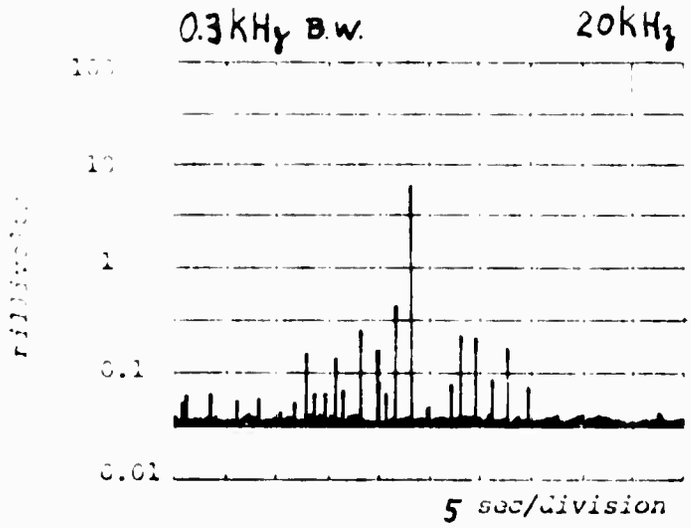

Figure 4. Emission output vs. time with a 20 KHz, 0.3 KHz bandwidth filter.

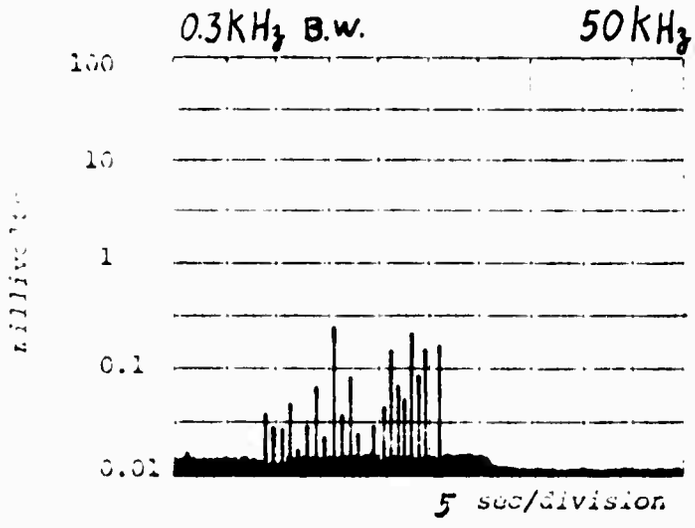

Figure 5. Emission output vs. time with 50 KHz, 0.3 KHz bandwith (B.W.) filter.

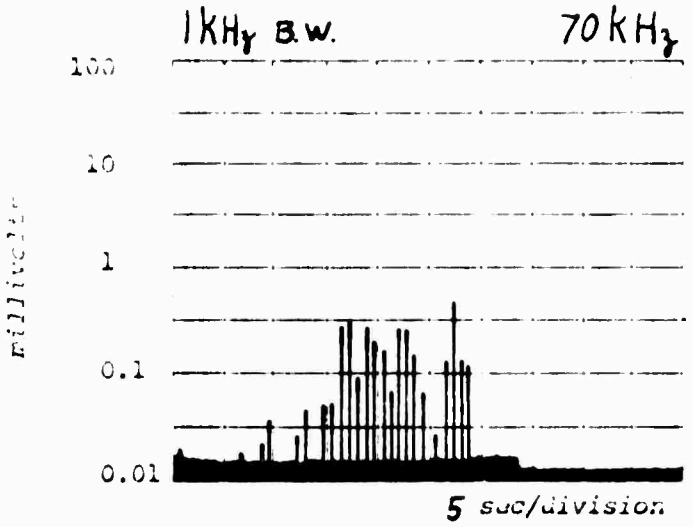

Figure 6. Emission output vs. time with a 70 KHz, 1 KHz B.W. filter.

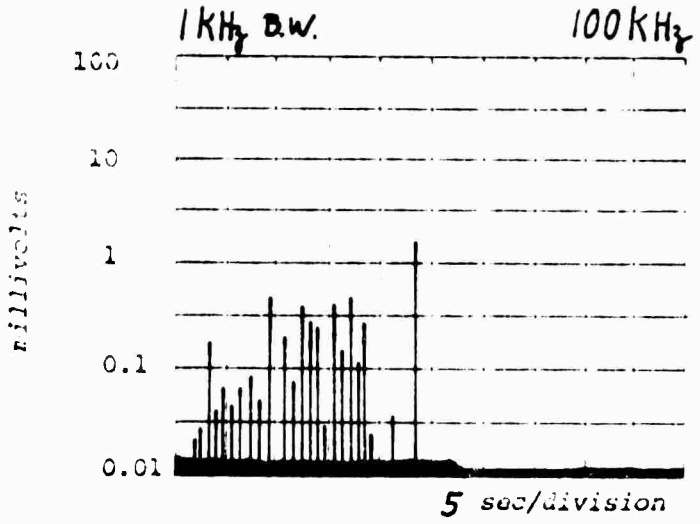

Figure 7. Emission output vs. time with a 100 KHz, 1 KHz B.W. filter.

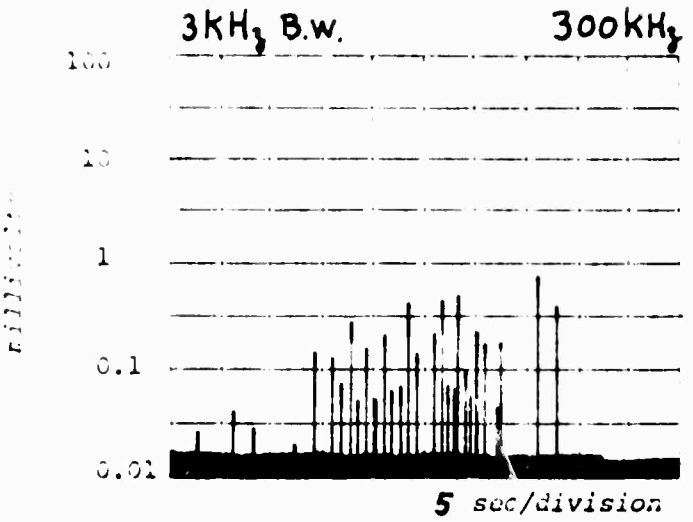

Figure 8. Emission output vs. time with a 300 KHz, 3 KHz B.W. filter.

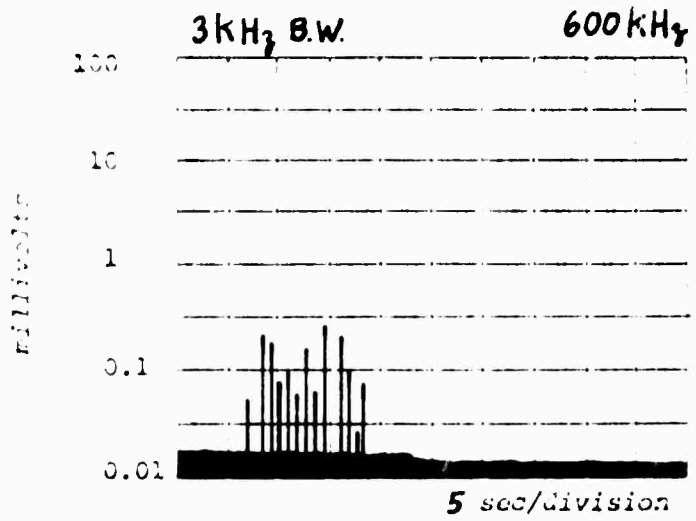

Figure 9. Emission output vs. time with a 600 KHz, 3 KHz B.W. filter.

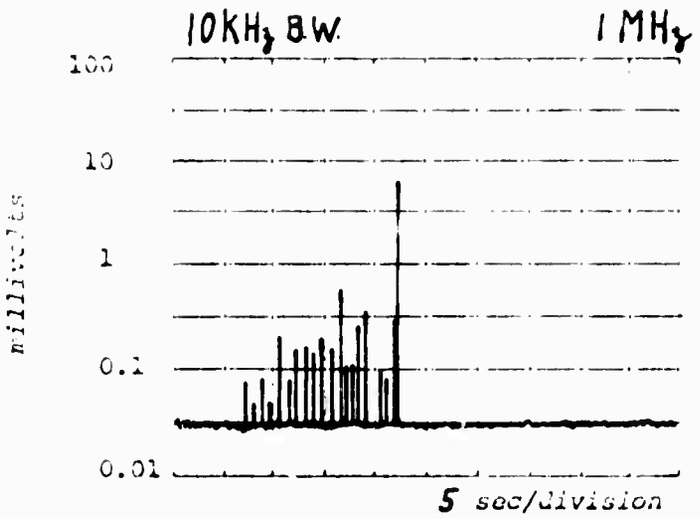

Figure 10. Emission output vs. time with a 1 MHz, 10 KHz B.W. filter.

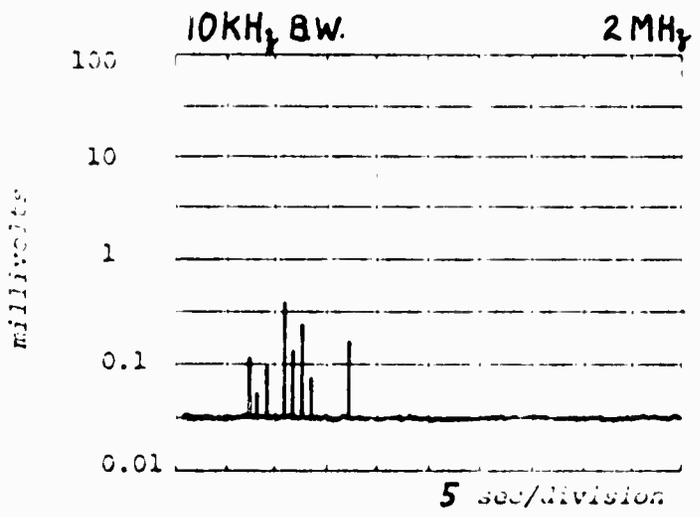

Figure 11. Emission output vs. time with a 2 MHz, 10 KHz B.W. filter.

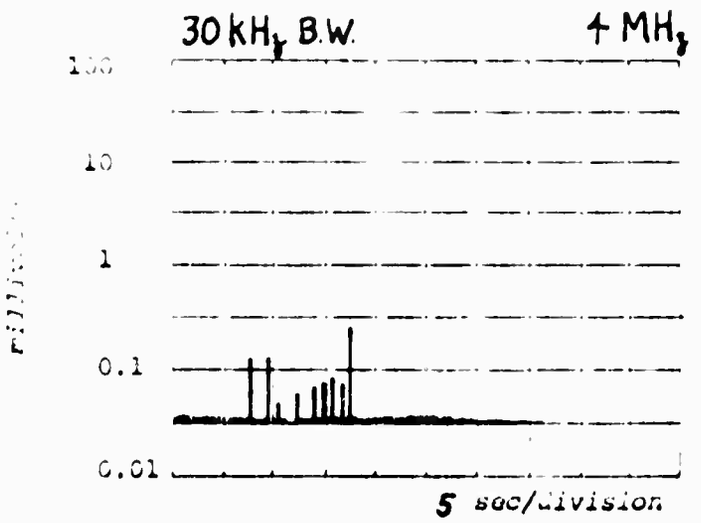

Figure 12. Emission output vs. time with a 4 MHz, 30 KHz B.W. filter.

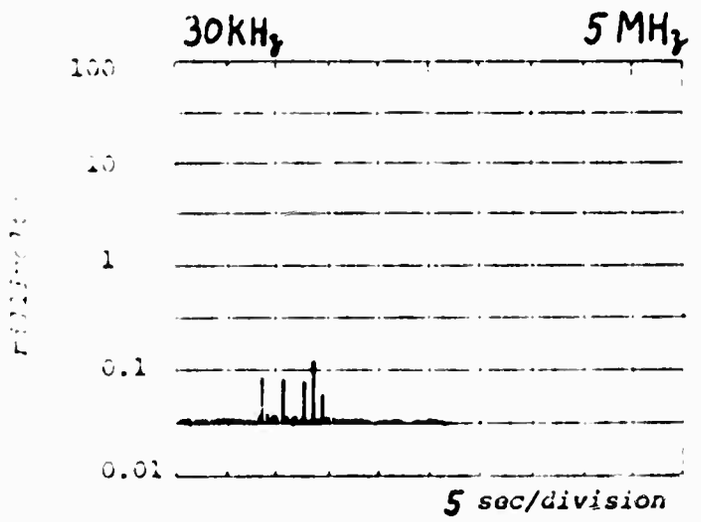

Figure 13. Emission output vs. time with a 5 MHz, 30 KHz B.W. filter.

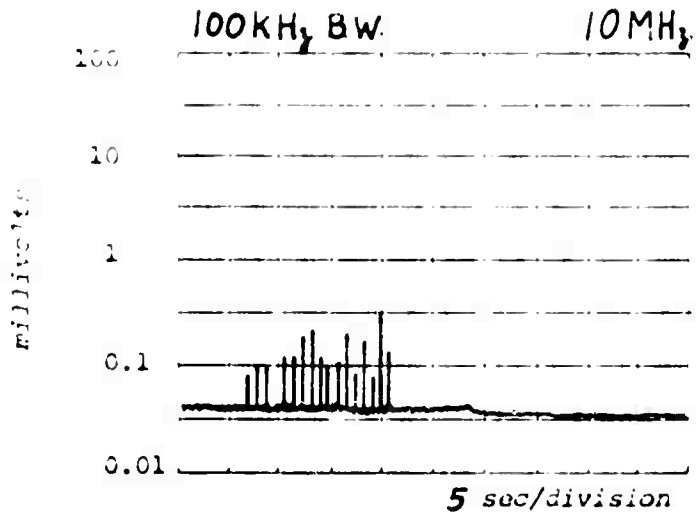

Figure 14. Emission output vs. time with a 10 MHz, 100 KHz B.W. filter.

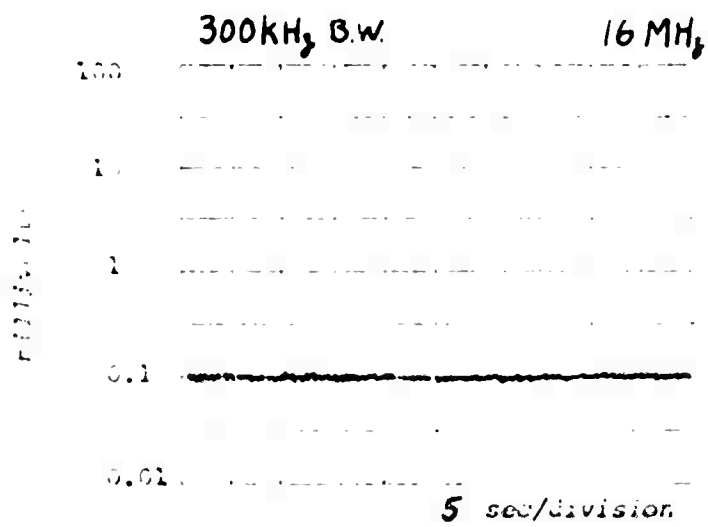

Figure 15. Emission output vs. time with a 16 MHz, 300 KHz B.W. filter.

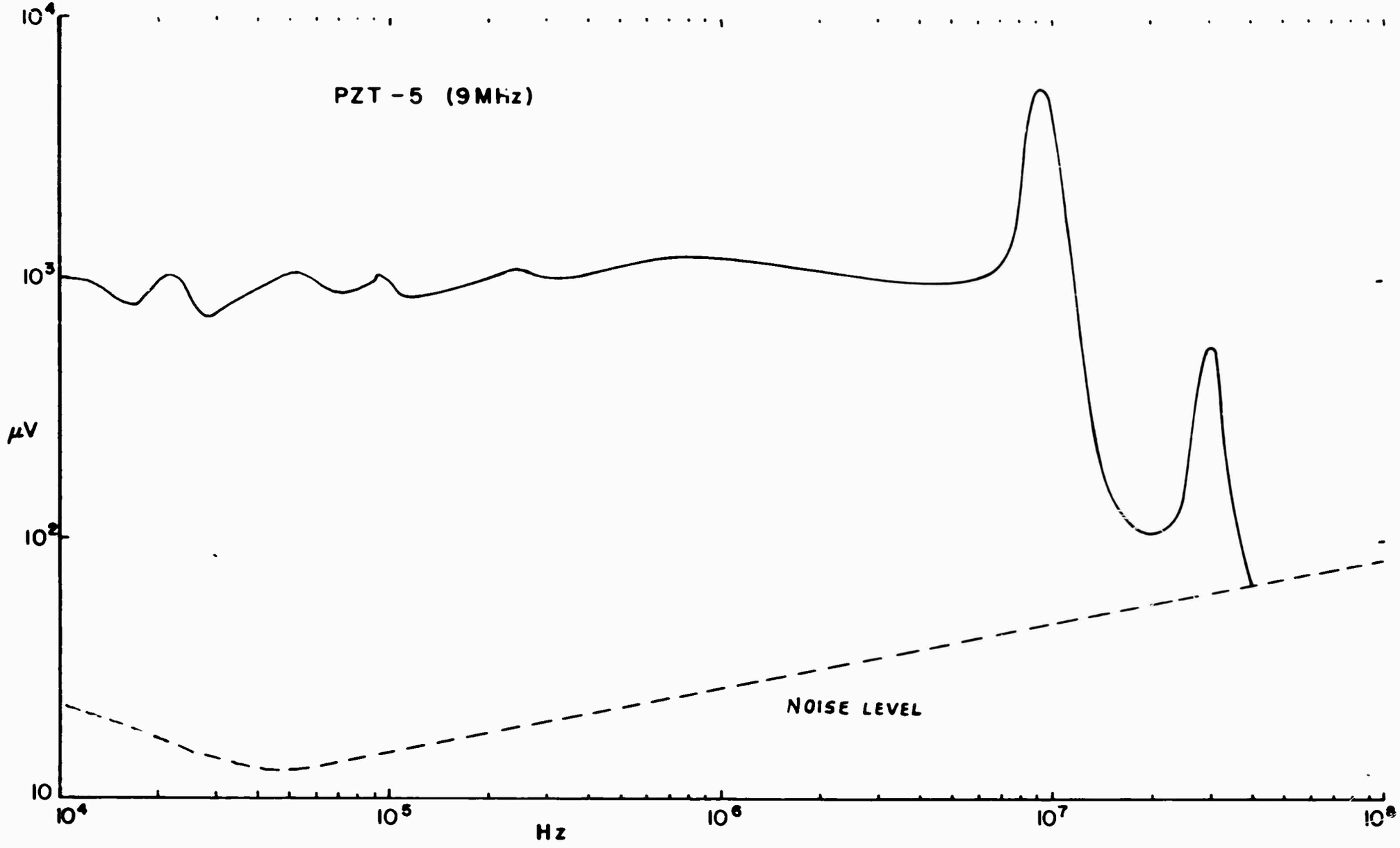

Figure 16. Spectral response of PZT-5 transducer used in this investigation.

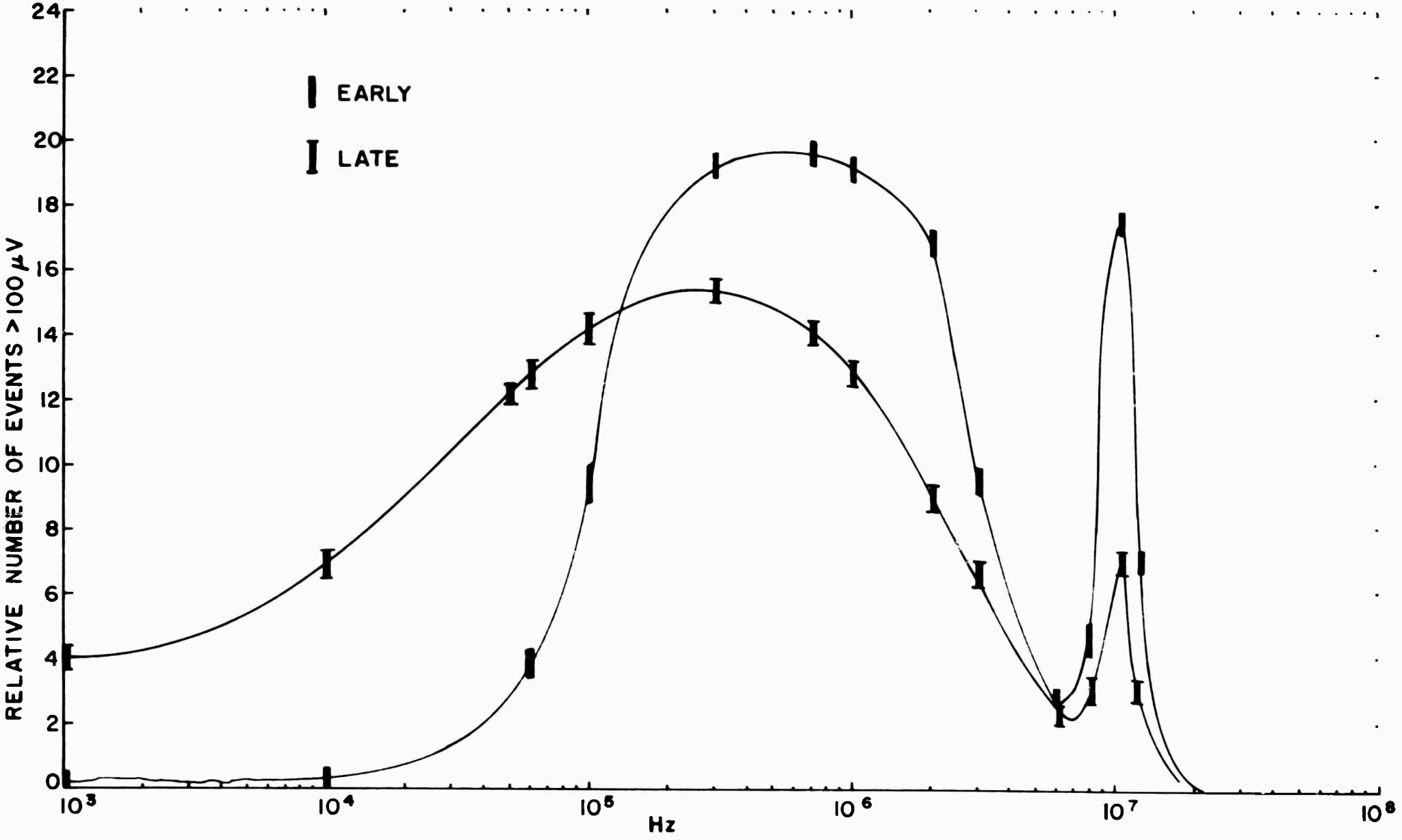

Figure 17. Spectrogram of acoustical emission output of high amplitude, low cycle fatigue specimens.

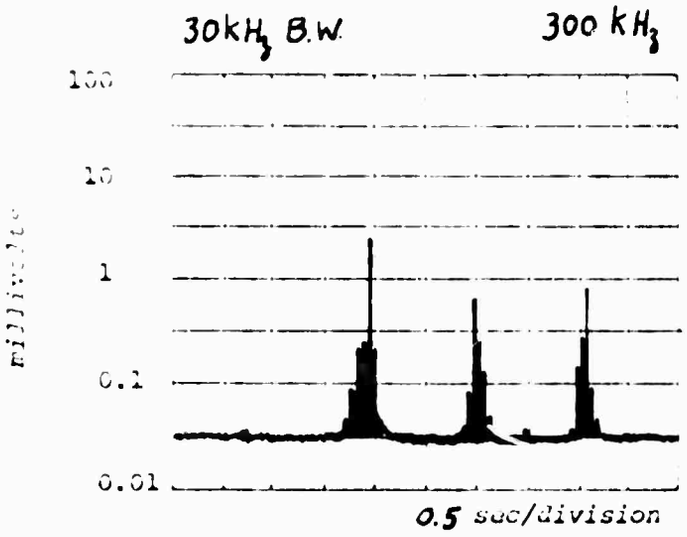

Figure 18. Acoustical emission output vs. time for early stage of cracking showing detail of time domain at 300 KHz.

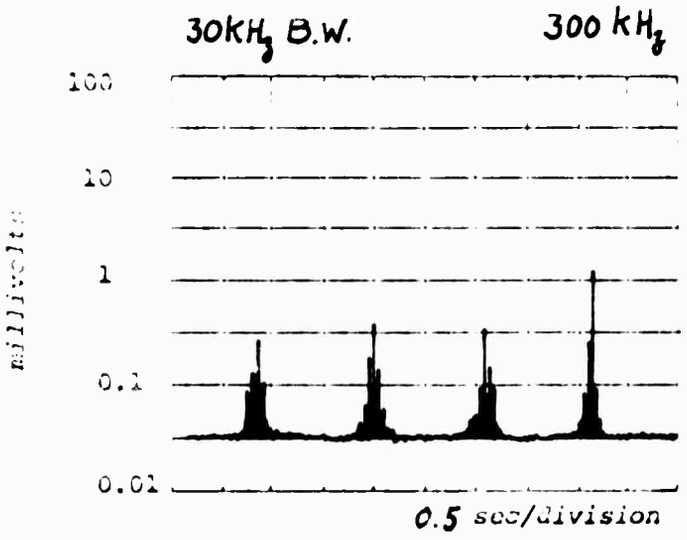

Figure 19. Emission output vs. time for slightly later stage of cracking than shown in Figure 18.

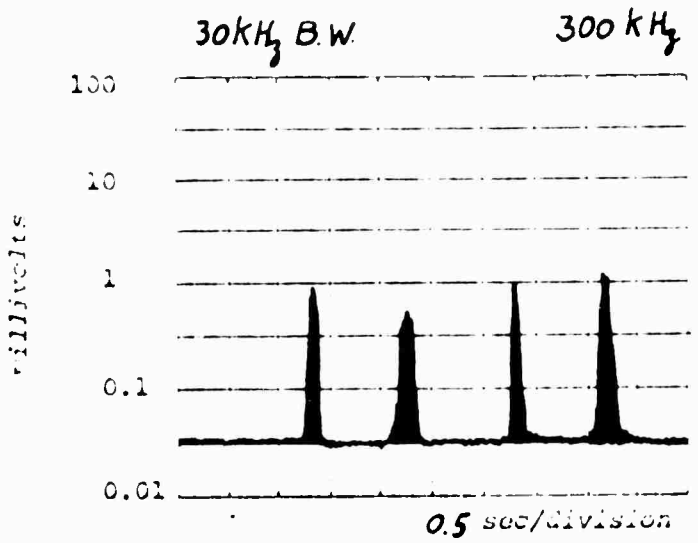

Figure 20. Emission output vs. time for still later stage of cracking.

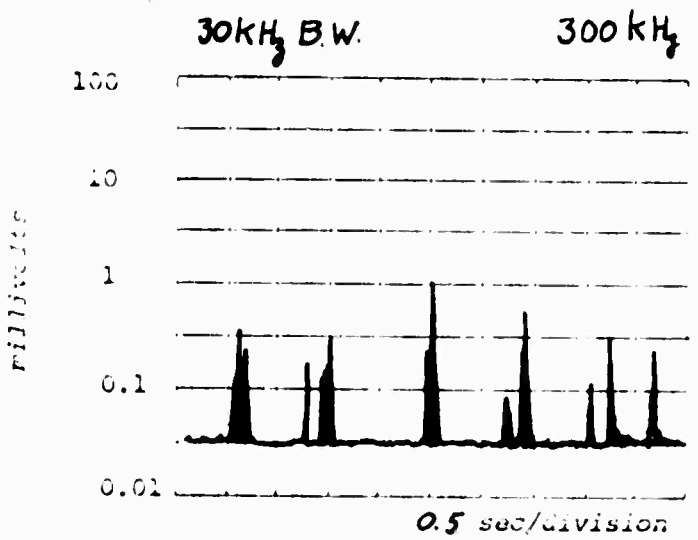

Figure 21. Emission output vs. time for nearly late stage of cracking. (Notice narrowing of time domain pulses.)

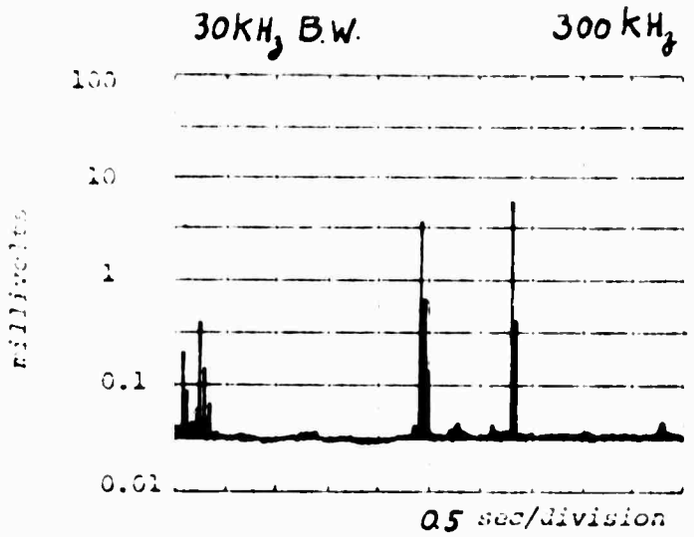

Figure 22. Emission output vs. time for late stage of cracking. Pulses have narrowed and increased in height compared to those in Figure 18.

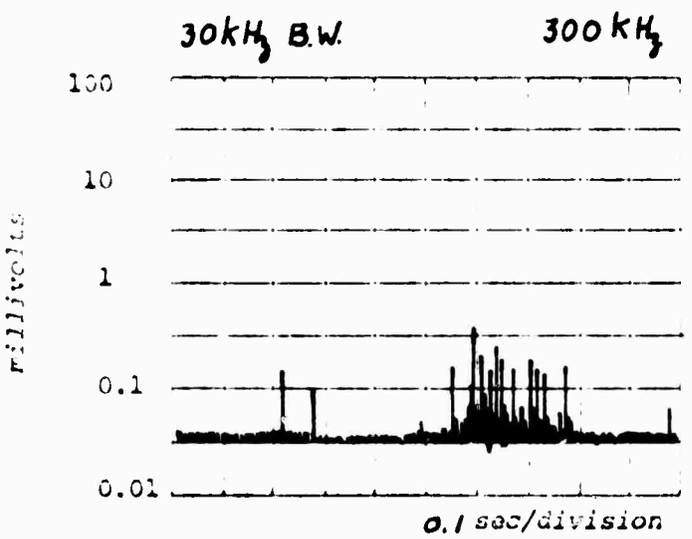

Figure 23. Emission output vs. time of early stage of cracking taken at a faster scope sweep rate to increase time resolution. (0.1 Sec/div.)

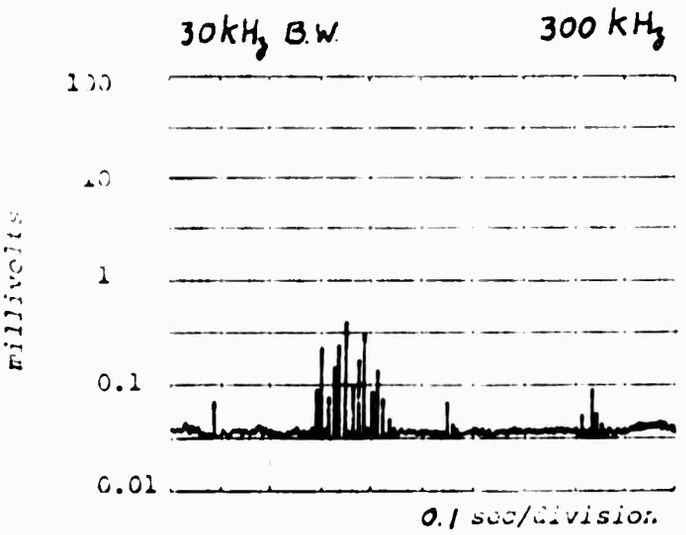

Figure 24. Emission output vs. time of slightly later stage of cracking than shown in Figure 23. (0.1 Sec/div.)

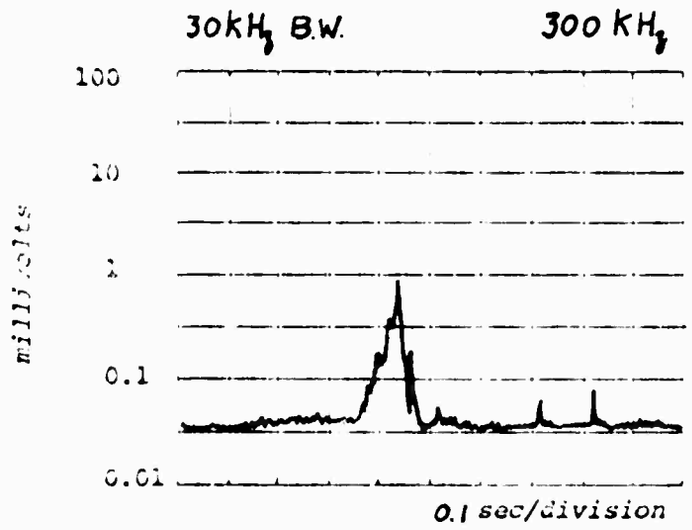

Figure 25. Emission output vs. time of still later stage (0.1 Sec/div.).

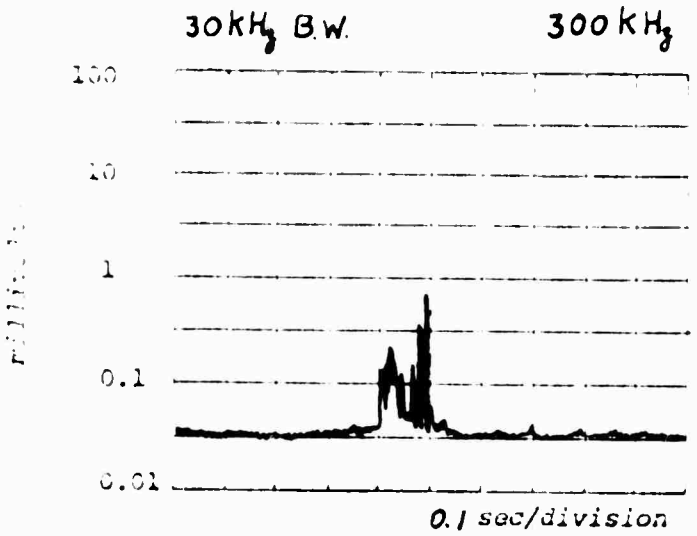

Figure 26. Emission output vs. time of late stage cracking (0.1 Sec/div.).

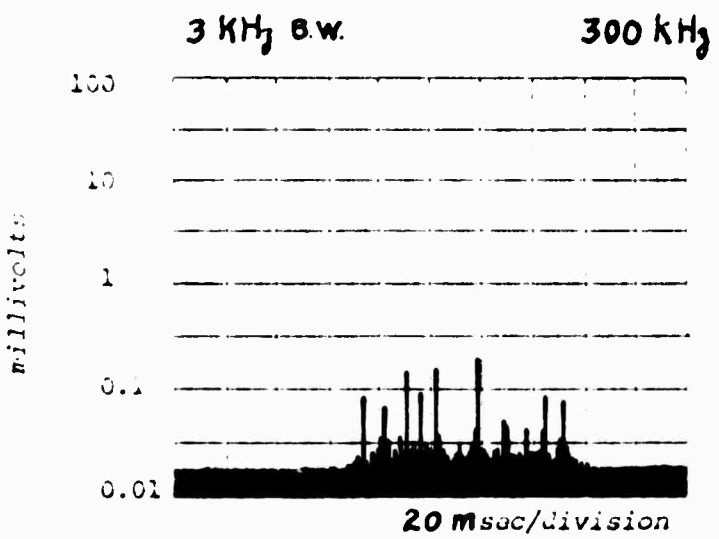

Figure 27. Emission output vs. time of late stage taken at even faster scope sweep rate (20 m Sec/div.) to increase time resolution still further.

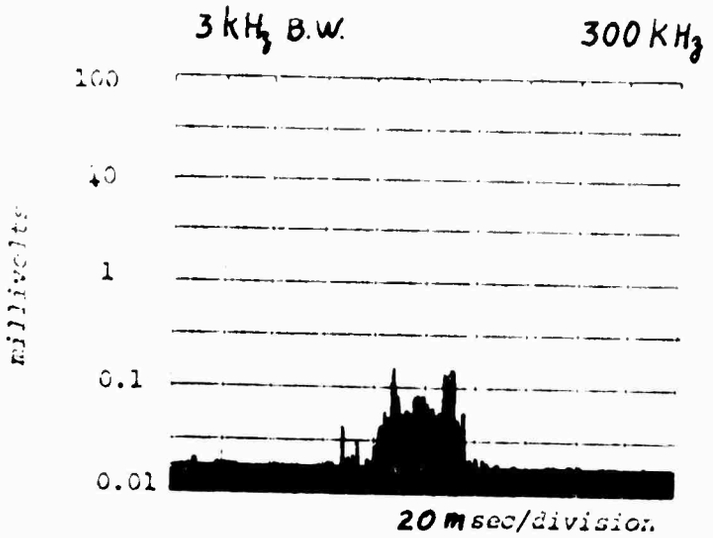

Figure 28. Emission output vs. time of very late stage near failure (20 m Sec/div.).

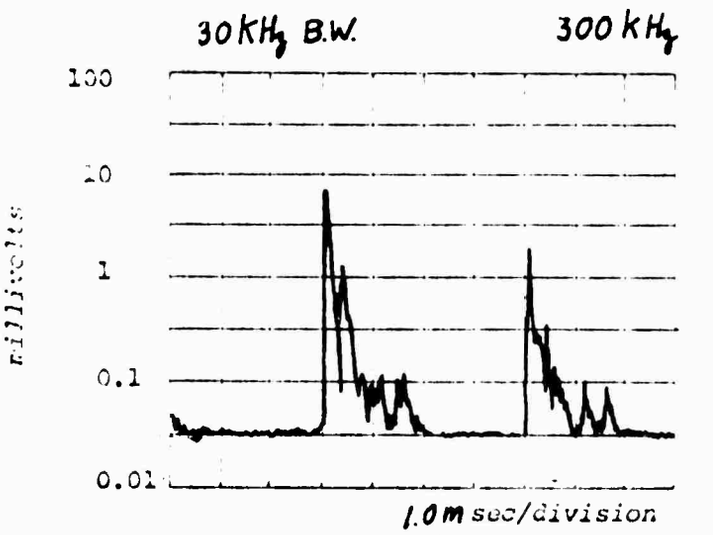

Figure 29. Emission output vs. time of events within ~5 cycles of failure taken at 20 times sweep rate of that in Figure 28. Ring down characteristic of damped specimen is now observed.

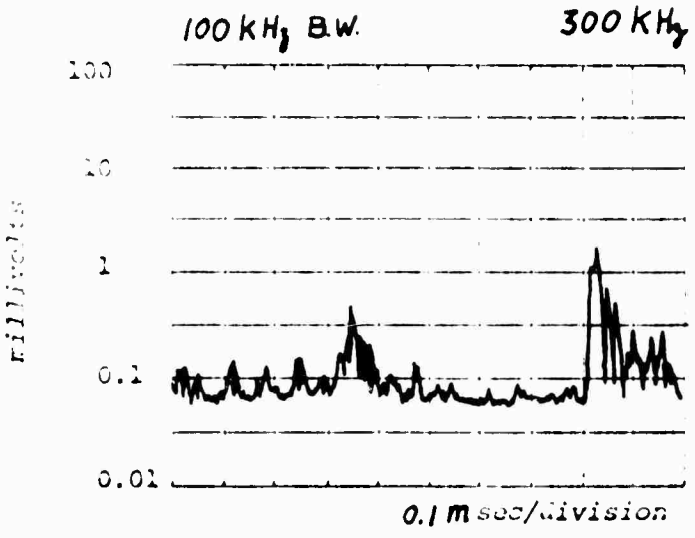

Figure 30. Emission output vs. time of terminal events taken at 0.1 m sec/div sweep rate. Bandwidth of filter centered at 300 KHz has been increased to 100 KHz.

EXO-ELECTRON EMISSION STUDIES

Stuart A. Hoenig

Co-Principal Investigator

Efforts during this period were devoted to investigating the post fatigue exo-electron emission from nickel wires. The work was done in a vacuum system at 10^{-8} torr to preclude oxidation effects from interfering with the measurement. The exo-electron emission was observed without ambient illumination by simply heating the fatigued specimens.

Typical data are shown in Figure 1. The exo-electron current is a clear measure of the fatigue level.

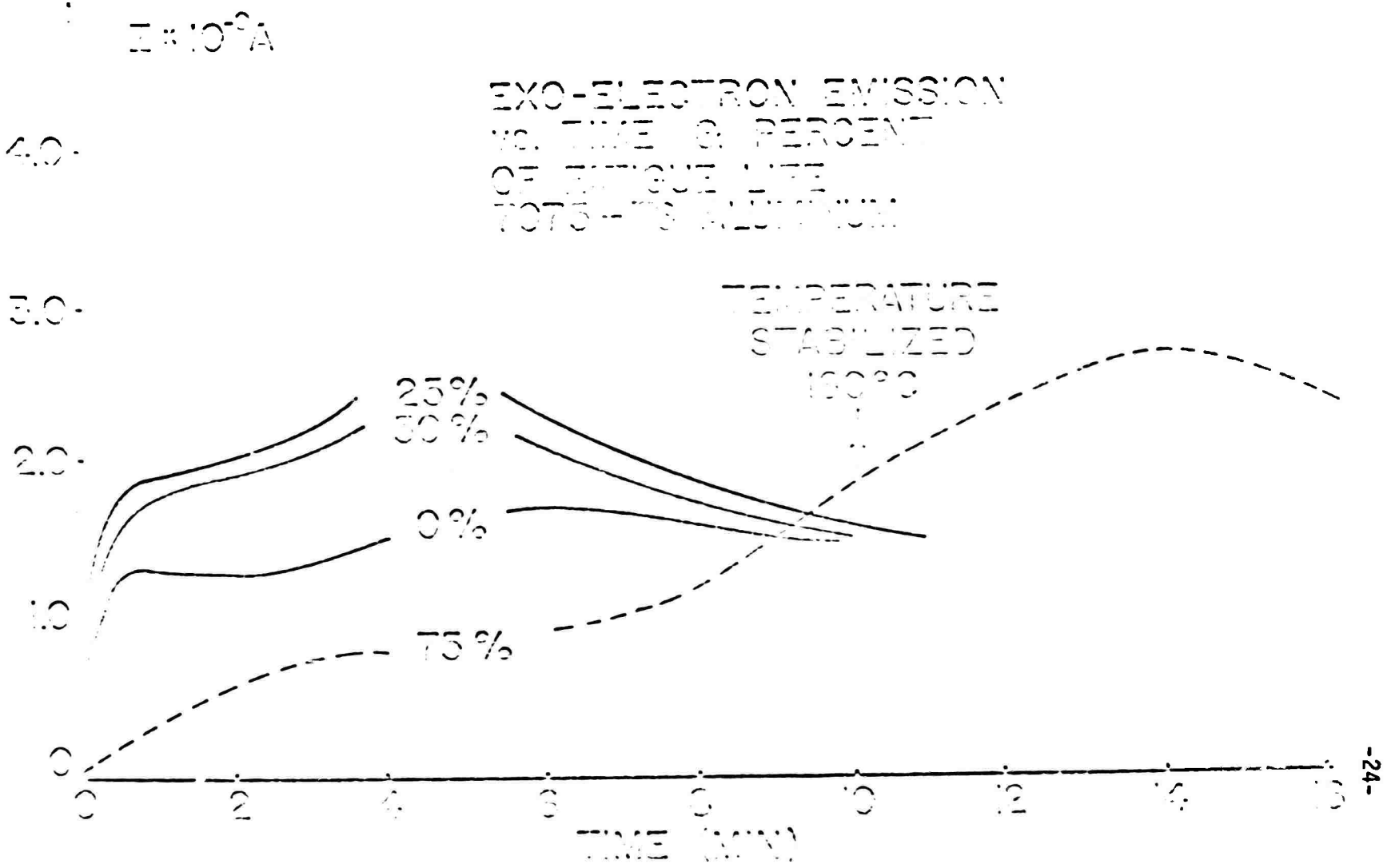

FIGURE 2